REVIEW

Action of antimicrobial peptides and cell-penetrating peptides on membrane potential revealed by the single GUV method

Md. Mizanur Rahman Moghal[1,2] · Farzana Hossain[1] · Masahito Yamazaki[1,3,4]

Abstract

Membrane potential plays various key roles in live bacterial and eukaryotic cells. So far, the effects of membrane potential on action of antimicrobial peptides (AMPs) and cell-penetrating peptides (CPPs) have been examined using cells and small lipid vesicles. However, due to the technical drawbacks of these experiments, the effect of membrane potential on the actions of AMPs and CPPs and the elementary processes of interactions of these peptides with cell membranes and vesicle membranes are not well understood. In this short review, we summarize the results of the effect of membrane potential on the action of an AMP, lactoferricin B (LfcinB), and a CPP, transportan 10 (TP10), in vesicle membranes revealed by the single giant unilamellar vesicle (GUV) method. Parts of the actions and their elementary steps of AMPs and CPPs interacting vesicle membranes under membrane potential are clearly revealed using the single GUV method. The experimental methods and their analysis described here can be used to elucidate the effects of membrane potential on various activities of peptides such as AMPs, CPPs, and proteins. Moreover, GUVs with membrane potential are more suitable as a model of cells or artificial cells, as well as GUVs containing small vesicles.

Keywords Single giant unilamellar vesicles · Antimicrobial peptides · Cell-penetrating peptides · Membrane potential · Artificial cells · Bio-imaging

Introduction

The resting membrane potential (φ_m) of all eukaryotic and bacterial cells has negative values ranging widely from −20 to −150 mV depending on cell type (Alberts et al. 2015; Sperelakis 2012). For example, the φ_m of animal cells ranges from −20 to −120 mV (Alberts et al. 2015). The φ_m of *Escherichia coli* cells ranges from −100 to −150 mV at pH 6.0~8.0, depending on pH (Felle et al. 1980). Membrane

potential plays a vital role in functions of membrane proteins such as voltage-gated ionic channels and ATP synthase (Hille 1992; Sperelakis 2012). Several studies have revealed that the φ_m also plays various key roles in plasma membranes. For example, in eukaryotic cells, cell proliferation (Blackiston et al. 2009; Sunderacruz et al. 2009), the location of lipids, the binding of proteins (Zhou et al. 2015), and the internalization of transporter from the cell membrane (Richardson et al. 2015) depend on φ_m greatly. In bacterial cells, the φ_m also affects significantly localization of membrane proteins and cell divisions (Strahl and Hamoen 2010; Kralj et al. 2011), secretion of proteins (Daniels et al. 1981), and proliferation (Stratford et al. 2019).

In this short review, we describe the effects of φ_m on the action of antimicrobial peptides (AMPs) and cell-penetrating peptides (CPPs). AMPs are natural peptides which kill bacterial cells or inhibit their growth. Almost all organisms including human release their specific AMPs as one of innate immune systems (Zasloff 2002; Yeaman and Yount 2003; Hancock and Hans-Georg 2006; Melo et al. 2009; Pasupleti et al. 2012; Propheter et al. 2017). The primary cause of the bactericidal activity of most AMPs is to increase plasma

✉ Masahito Yamazaki
yamazaki.masahito@shizuoka.ac.jp

1 Integrated Bioscience Section, Graduate School of Science and Technology, Shizuoka University, Shizuoka 422-8529, Japan

2 Present address: Department of Pharmacy, Mawlana Bhashani Science and Technology University, Tangail 1902, Bangladesh

3 Nanomaterials Research Division, Research Institute of Electronics, Shizuoka University, 836 Oya, Suruga-ku, Shizuoka 422-8529, Japan

4 Department of Physics, Faculty of Science, Shizuoka University, Shizuoka 422-8529, Japan

membrane permeability, which exposes the contents of their cytoplasm (Zasloff 2002; Melo et al. 2009; Sochacki et al. 2011). AMPs comprising D-amino acids exhibit similar antimicrobial activities (Bobone and Stella 2019), indicating that AMPs target the lipid bilayer regions of bacterial cell membranes. The action of AMPs involves selective binding and damage to plasma membranes. The mechanism of binding is well understood; AMPs are highly cationic peptides and bind selectively to bacterial cells because their outer leaflet is more negatively charged (Zasloff 2002). Table 1 shows the amino acid sequence and structure in lipid bilayers of two typical AMPs, lactoferricin B (LfcinB) and magainin 2. However, the mechanisms of AMP-induced damage are not well-known, although several models have been proposed (Zasloff 2002; Melo et al. 2009). We consider that the φ_m may play a key role in the AMP-caused damage of cell membranes because all bacterial cells have large negative membrane potentials.

On the other hand, CPPs are natural peptides and artificial peptides that enter the cytoplasm of eukaryotic cells without decreasing their viability. This characteristic enables CPPs to be used for delivery of drugs and oligonucleotide into the cytosol of live cells (Zorko and Langel 2005; Madani et al. 2011; Bechara and Sagan 2013; Stanzl et al. 2013). Table 1 shows the amino acid sequence and structure in lipid bilayers of two typical CPPs, transportan 10 (TP10) and nona-arginine (R_9) (one of oligoarginine). CPPs enter the cytoplasm via several routes, such as various endocytic pathways using vesicles originated from plasma membrane (e.g., endosomes) and direct translocation across plasma membranes. Irrespective of routes, it is essential for CPPs to translocate across the membranes. These membranes have a membrane potential φ_m, and thus, CPPs may use this for their entry.

Previous studies on the effect of φ_m on AMPs and CPPs

The effects of φ_m on action of AMPs and CPPs have been examined using cells and small lipid vesicles. Interaction of AMPs with different strains of bacteria with different membrane potentials suggests that the AMP activity is greater for larger negative membrane potential (Yeaman et al. 1998). The effects of the increase in K^+ concentration in aqueous solution outside eukaryotic cells on the entry of CPPs into their cytosol have been studied, and the results suggest that the efficiency of entry of CPPs decreases with a decrease in negative membrane potential (Rothbard et al. 2004, 2005; Henriques et al. 2005). An opposite result was also reported, namely, that entry of a CPP, nona-arginine (R_9) into cells, does not depend on membrane potential (Wallbrecher et al. 2017). Similar experiments have been performed for AMPs, and the results suggest that activities of some AMPs decrease with a decrease in negative membrane potential (Wu et al. 1999). However, as described above, the change in membrane potential alters greatly the organization of membrane proteins and lipids in the plasma membranes, and hence, many factors can be involved in the causes for the change in activities of AMPs and CPPs.

On the other hand, the interactions of CPPs with lipid vesicles have been studied using suspensions of large unilamellar vesicles (LUVs) (Terrone et al. 2003; Zhang et al. 2009). The results suggest that the number of fluorescent dye-labeled CPPs entered LUVs increases in the presence of φ_m. However, we cannot observe each LUV interacting with CPPs using the LUV suspension method, which provides only ensemble average of physical quantities (e.g., fluorescence intensity) of all LUVs at different stages in the suspension. These characteristics of the LUV suspension method conceal the elementary steps of the entry of CPPs (Yamazaki 2008; Islam et al. 2018). Moreover, there are some difficulties in

Table 1 Typical AMPs and CPPs (amino acid sequence, structure, and orientation in membrane interface)

	Name	Amino acid sequence	Structure in membrane interface	Orientation in the membrane interface
AMP	Lactoferricin B (LfcinB)	FKCRRWQWRMKKLGAPSITCVRRAF (25 aa) (Bellamy et al. 1992)	Distorted antiparallel β-sheet with a disulfide bond (Hwang et al. 1998)	Amphiphatic 3D structure (Hwang et al. 1998)
AMP	Magainin 2	GIGKFLHSAKKFGKAFVGEIMNS (23 aa) (Zasloff 1987)	α-helix (Gesell et al. 1997)	Amphipathic α-helix parallel to the membrane surface (tilt angle[**] of helix is 90°) (Bechniger et al. 1993)
CPP	Transportan 10 (TP10)	AGYLLGKINLKALAALAKKIL (21 aa) (Soomets et al. 2000)	α-Helix (C-terminal region) and flexible structure (N-terminal region). 56% α-helix (Fanghänel et al. 2014)	Tilt angle[**] of amphipathic α-helix is 55° (Fanghänel et al. 2014)
CPP	Nona-arginine (R_9)	RRRRRRRRR (9 aa) (Futaki et al. 2001)	Random coil	ND

[**] The tilt angle between the helix axis and the bilayer normal

estimation of entrapment of fluorescent dye-labeled CPPs using the LUV suspension method (Islam et al. 2018). Planar lipid bilayers have been used for this purpose, which provide information on AMPs which form ionic channels, but not other types of AMPs (Christensen et al. 1988; Kagan et al. 1990; Wu et al. 1999; Hancock and Rozek 2002). Moreover, it is difficult to elucidate the elementary steps of action of AMPs.

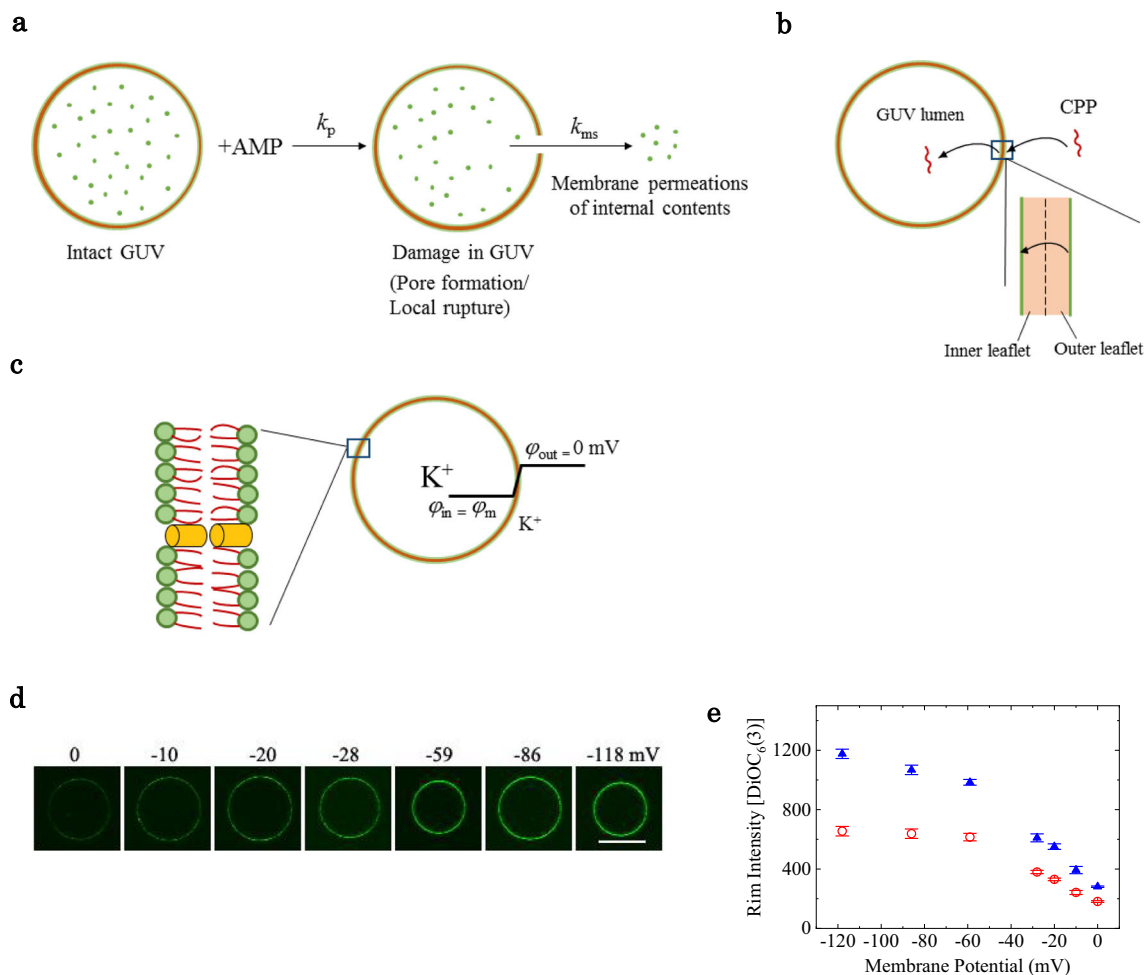## The action of AMPs and CPPs using the single GUV method

In the single giant unilamellar vesicle (GUV) method, we can observe the interaction of substances such as peptides, proteins, and physiologically active substances with a single GUV under various optical microscopes. Thus, the single GUV method enables to separate elementary steps in peptide/protein-induced reaction in individual GUVs. From the statistical analysis of changes in physical quantities of single GUVs, we can determine the rate constant or a measure of the rate of each elementary steps of the interactions (Yamazaki 2008; Islam et al. 2014b). For example, in the AMP-induced leakage of GUV contents, two important elementary steps, i.e., the AMP-caused damage in the membrane such as pore formation and local rupture and the following membrane permeation of internal contents through the damage, can be separated, and their rate constants have been obtained (Fig. 1a) (Tamba and Yamazaki 2005, 2009; Tamba et al. 2010; Karal et al. 2015). These two steps are induced by completely different physical factors; for example, the size and the number of pores or local ruptures determine the rate of the membrane permeation. On the other hand, the LUV suspension method cannot separate the processes, and hence, only the ensemble average of membrane permeation from LUVs at different states is obtained. For the entry of CPPs into GUV lumen, the binding of fluorescent dye-labeled CPPs to the outer leaflet of the GUV membrane from aqueous solution, their translocation from the outer leaflet to the inner one of the membrane, and the unbinding of CPPs from the inner leaflet to the aqueous solution in the GUV lumen can be separated and their rates are estimated (Fig. 1b) (Islam et al. 2014a, 2017; Sharmin et al. 2016; Moghal et al. 2018). Simultaneous measurement of entry of CPPs into the GUV lumen and the membrane permeation of internal contents using confocal laser scanning microscopy (CLSM) can reveal the relationship between the entry of CPPs and the CPP-caused pore formation (Islam et al. 2014a, 2017; Moghal et al. 2018). The time course of change in fluorescence intensity (FI) of a GUV membrane (i.e., rim intensity) due to fluorescent dye-labeled CPPs provides information on time course change in peptide concentration in the GUV membrane, which has revealed the time course of translocation of

peptides across lipid bilayer (Islam et al. 2014a, 2017; Karal et al. 2015). On the other hand, the membrane tension in single GUVs can be accurately controlled by the micropipette aspiration method and the osmotic pressure, and thus, we can elucidate the effect of membrane tension on the action of AMPs and CPPs (Karal et al. 2015; Shibly et al. 2016; Islam et al. 2017; Hasan et al. 2018, 2019). Other important characteristics of the single GUV method have been discussed previously (Tamba et al. 2007; Islam et al. 2014b, 2018; Hasan and Yamazaki 2019; Hasan et al. 2019).

For the single GUV method, GUVs are prepared by the natural swelling method and then purified using the membrane filtering method (Tamba et al. 2011). There are various preparation methods of GUVs, but for studying the interactions of peptides/proteins with GUVs, it is important to prepare GUVs without oils, because residual oil in the GUVs membrane prepared using oil affects physical properties of the membranes (Walde et al. 2010). For example, in the GUVs prepared by the water-in-oil emulsion transfer method (Pautot et al. 2003), membrane permeability of calcein (a water-soluble negatively charged fluorescent dye) is high (Lin et al. 2018).

Application of φ_m to single GUVs

In the current method for application of φ_m to GUVs, the membrane contains a low concentration of gramicidin A (monovalent cation channel) (Finkelstein and Andersen 1981; Hille 1992), and K^+ concentration difference is produced between the inside and the outside of the GUVs (Fig. 1c) (Hossain et al. 2019; Moghal et al. 2020). To adjust the osmotic pressure, we use tetraethylammonium ion (TEA^+) so that the sum of K^+ and TEA^+ concentrations in aqueous solution outside the GUVs equals to K^+ concentration in the GUV lumen, because it is known that TEA^+ cannot pass through the gramicidin A channel without its blocking (Andersen 1983). The membrane potential in cells has been estimated by a φ_m-sensitive fluorescent dye, $DiOC_6(3)$ (Shapiro 1994; Ishihara and Shimamoto 2006). Figure 1 d and e show that the rim intensity, I_{rim}, due to $DiOC_6(3)$ is raised with an increase in negative membrane potential (or $|\varphi_m|$), calculated by the Nernst equation. This result can be explained by the increase in $DiOC_6(3)$ concentration in the inner leaflet of the GUV membrane due to φ_m. Quantitative analysis indicates that the φ_m dependence of the I_{rim} at and below −28 mV agreed with the theory based on the Boltzmann distribution of the dye between outer and inner leaflet (Moghal et al. 2020). The I_{rim} due to $DiOC_6(3)$ does not change for at least 1 h, indicating that the φ_m in the GUV is stable for a long time.

a

b

c

d

e

Fig. 1 Elementary processes of action of AMPs and CPPs and application of membrane potentials to GUVs. **a** A diagram of elementary steps of action of AMPs. **b** A diagram of entry of CPPs into single GUV lumen. **c** A diagram of the method of application of membrane potentials. **d** The φ_m dependence of I_{rim} due to $DiOC_6(3)$ in PG/PC (2/8)-GUVs. CLSM images of the GUVs interacting with 2 nM $DiOC_6(3)$ under various values of φ_m, which is denoted by the number above each image. The bar denotes 20 μm. **e** The φ_m dependence of I_{rim} due to $DiOC_6(3)$. (red circle) 1-nM and (blue triangle) 2-nM $DiOC_6(3)$. The error bars denote SE values of I_{rim}. **d** and **e** are reprinted from Moghal et al. (2020) with permission from American Biophysical Society

Effect of φ_m on AMP-caused damage of GUV membrane

Here we summarize the results of the effect of φ_m on the action of an AMP, lactoferricin B (LfcinB), which is a hydrolyzed fragment of bovine lactoferrin by trypsin (Bellamy et al. 1992; Kuwata et al. 1998). Previous studies using the single GUV method indicate that in the interaction of LfcinB with single GUVs composed of a dioleoylphosphatidylglycerol (DOPG) and dioleoylphosphatidylcholine (DOPC) mixture, LfcinB induces local rupture in single GUVs stochastically, resulting in rapid membrane permeation of calcein (Moniruzzaman et al. 2015). This rapid membrane permeation is different from the gradual membrane permeation of calcein via magainin 2-caused pores in lipid bilayers (Tamba and Yamazaki 2009). LfcinB also induces membrane permeation of calcein from single *E. coli* cells stochastically, for example,

with 5-μM LfcinB, all examined single cells show membrane permeation of calcein with various rates within 6 min (Hossain et al. 2019). However, 5-μM LfcinB cannot induce membrane permeation of fluorescent dye, Alexa Fluor 647 hydrazide (AF647), from most single GUVs comprising *E. coli* polar lipid extract (*E. coli*-lipid: phosphatidylethanolamine (PE)/phosphatidyl glycerol (PG)/cardiolipin (CA) [67/ 23/10 (wt% ratio)]). To elucidate this discrepancy, the effect of φ_m on the interaction of LfcinB with single *E. coli*-lipid-GUVs was studied using CLSM (Hossain et al. 2019).

Figure 2a shows the interaction of 5-μM LfcinB with a single *E. coli*-lipid-GUV containing AF647 at $\varphi_m = -102$ mV. The continuous addition of LfcinB solution to the neighborhood of the GUV using a micropipette is started from $t = 0$. Initially, the FI of the GUV lumen (i.e., lumen intensity), I_{lumen}, due to AF647, does not change, and from 50 s the I_{lumen} rapidly decreases to zero (Fig. 2a). After that, the structure of

GUV changes (its size decreases and the rim of the GUV becomes inhomogeneous), indicating that LfcinB induces local rupture of the GUV membrane, through which rapid membrane permeation of AF647 occurs. Figure 2b shows the time course change in I_{lumen} of several "single GUVs," indicating that the starting time of rapid decrease in I_{lumen}, i.e., the time of local rupture, is random, but the rate of decrease in I_{lumen} after the local rupture (i.e., the rate of membrane permeation of AF647) is almost the same in all examined GUVs. To analyze the stochastic AMP-caused pore formation or local rupture in lipid bilayer, we plot the time course of the fraction of intact GUVs with no membrane permeation of fluorescent dye among all examined GUVs, P_{intact} (t) (Tamba and Yamazaki 2005, 2009). Figure 2c shows that the P_{intact} of GUVs under this condition decreases with time to zero, indicating that

within 8 min interaction local rupture occurs in all examined GUVs. The time course of P_{intact} is well fit by a theoretical equation (P_{intact} = exp {$-k_p$ (t - t_{eq})}) for the two-state transition from the intact GUV to the locally ruptured GUV, where k_P is the rate constant of the LfcinB-caused local rupture and t_{eq} is a fitting parameter. From this fitting, the value of k_P is determined. For the same concentration of LfcinB, the k_P increases with $|\varphi_m|$ (Fig. 2d). If we use the fraction of leaked GUV among all examined GUVs at a specific interaction time, P_{leak} (t) (= 1 − P_{intact} (t)), we can estimate the lower rate of AMP-caused pore formation or local rupture even if the k_P value cannot be determined (Tamba and Yamazaki 2005, 2009). Figure 2e shows the LfcinB concentration dependence of P_{leak} (10 min) of GUVs under φ_m = − 102 mV and 0 mV, indicating clearly that lower concentrations of LfcinB induces
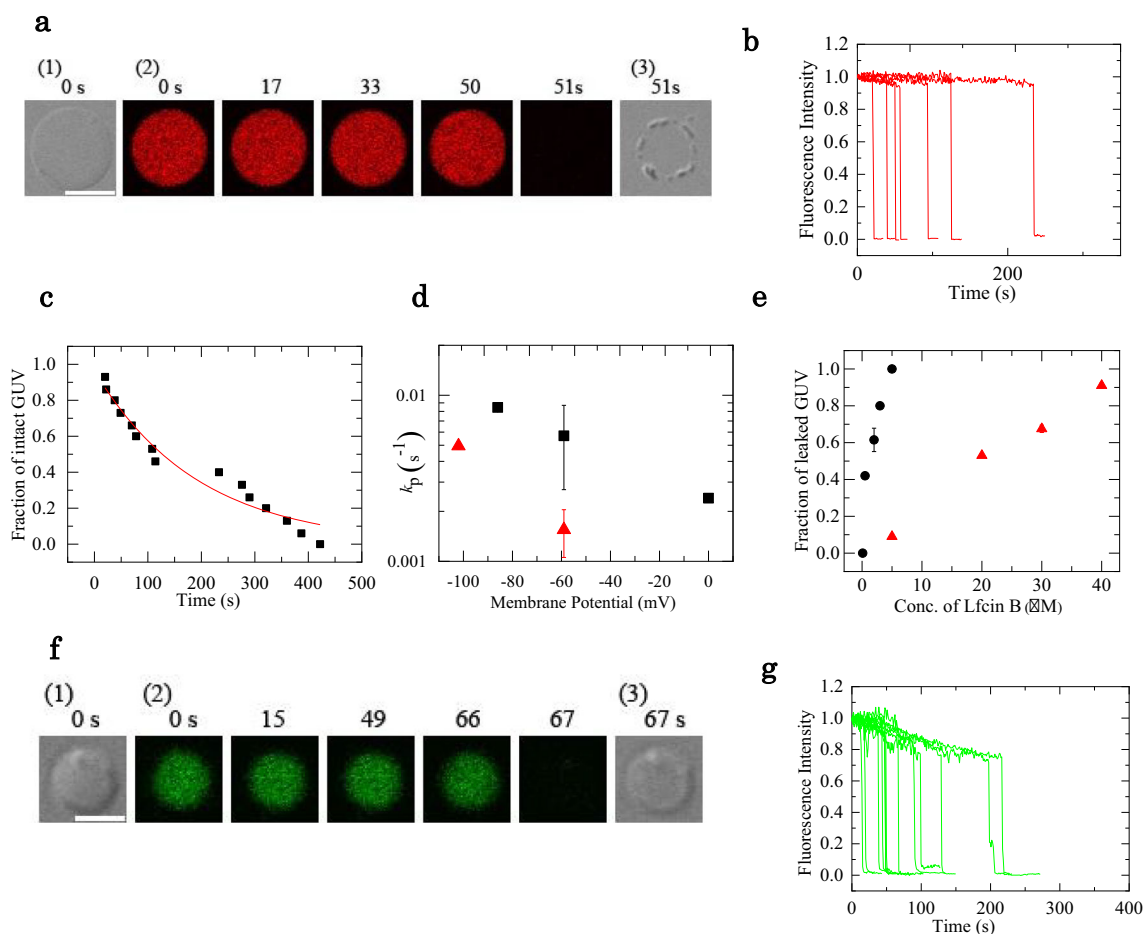
Fig. 2 LfcinB-caused membrane permeation of fluorescent probes from single E. coli-lipid-GUVs and single E. coli spheroplasts under φ_m. **a** Membrane permeation of AF647 from single E. coli-lipid-GUVs with φ_m = − 102 mV induced by 5-μM LfcinB at 25 °C. CLSM images due to (2) AF647 and (1)(3) DIC. The interaction time of LfcinB with a GUV is denoted by the numbers above each image. The bar denotes 20 μm. **b** Time course change in I_{lumen} due to AF647 of several "single GUVs" under the same conditions used in **a**. Each curve represents the time course of each GUV. **c** Time course of P_{intact} of the experiments shown in **b**. The solid line represents the best fit curve of the equation in the text.

d The φ_m dependence of k_P. The error bars denote SDs of k_P (red triangle) 5 μM and (black square) 20-μM LfcinB. **e** LfcinB concentration dependence of P_{leak} (10 min) of GUVs under φ_m = − 102 mV (black circle) and 0 mV (red triangle). **f** Interactions of 2.0-μM LfcinB with single E. coli spheroplasts containing calcein. CLSM images due to (2) calcein and (1) (3) DIC. The interaction time of LfcinB with a spheroplast is denoted by the numbers above each image. The bar denotes 5.0 μm. **g** Time course change in I_{lumen} due to calcein of several spheroplasts during the interaction of 2.0-μM LfcinB at 25 °C. **a,b,c,d**, **e**, **f**, and **g** are reprinted with some modifications from Hossain et al. (2019)

local rupture of GUVs at $\varphi_m = -102$ mV. In contrast, the rate of membrane permeation of AF647 after local rupture at $\varphi_m = -102$ mV is almost the same as that at 0 mV (Hossain et al. 2019). These results indicate that the φ_m increases the rate constant of LfcinB-caused local rupture but does not change the rate constant of membrane permeation of AF647.

Effect of φ_m on AMP-caused damage of spheroplast membrane

We can investigate the interaction of peptides with single spheroplasts of bacterial cells using the similar method of the single GUV method (Hossain et al. 2019). Spheroplasts are prepared from bacterial cells by removing their outer membrane and peptidoglycan, and thus, spheroplasts have only cell membrane and cytoplasm, which is useful for investigation of bacterial cell membranes (Ruthe and Adler 1985; Martinac et al. 1987; Wei et al. 2016; Sun et al. 2016). Calcein is loaded in spheroplast cytoplasm by interacting calcein acetoxymethyl (calcein-AM) with spheroplasts using a similar method applied for *E. coli* cells (Dubey and Ben-Yehuda 2011; Moniruzzaman et al. 2017). Figure 2f shows the interaction of 2-μM LfcinB with a single *E. coli*-spheroplast containing calcein, indicating that a rapid membrane permeation of calcein occurs at 66 s, but consequently the apparent structure of the spheroplast does not change (Hossain et al. 2019). Figure 2g shows the time course change in I_{lumen} due to calcein of several "single spheroplasts," indicating that random, rapid decrease in I_{lumen} occurs although a small gradual decrease in I_{lumen} before rapid decrease occurs due to photobleaching of calcein. These data indicate that LfcinB induces a local rupture or large pore formation in the plasma membranes, resulting in rapid membrane permeation of calcein, which is similar to the phenomenon observed in GUVs. It is well-known that a proton ionophore, carbonyl cyanide *m*-chloro-phenylhydrazone (CCCP), decreases the membrane potential of cells (Strahl and Hamoen 2010). The presence of CCCP inhibits the LfcinB-caused membrane permeation of calcein from single *E. coli*-spheroplasts, indicating that the φ_m plays a key role in LfcinB-caused damage of cell membrane (Hossain et al. 2019).

Effect of φ_m on entry of CPPs into single GUV lumen

Next, we summarize the results of the effect of φ_m on the action of a CPP, transportan 10 (TP10) (Soomets et al. 2000; EL-Andaloussi et al. 2005). Previous studies using the single GUV method indicate that the interaction of higher concentrations of carboxyfluorescein (CF)-labeled TP10 (CF-TP10) (≥ 0.6 μM) with single DOPG/DOPC-GUVs induces its entry

into their GUV lumen without or before pore formation (Islam et al. 2014a; Moghal et al. 2018). To elucidate the effect of φ_m on the entry of CF-TP10, the interaction of lower concentrations of CF-TP10 with single DOPG/DOPC-GUVs was examined using CLSM (Moghal et al. 2020). Figure 3a shows the interaction of 0.50-μM CF-TP10 with a single DOPG/ DOPC (2/8)-GUVs containing AF647 and 1.2-mM LUVs (~ 100 nm diameter) in the GUV lumen at $\varphi_m = -59$ mV. After the interaction of CF-TP10 with the GUV starts, the I_{lumen} due to AF647 does not change for 6 min (Figs. 3a (1) and 3c), indicating that CF-TP10 does not cause pore formation in the GUV membrane. In contrast, the rim intensity, I_{rim}, due to CF-TP10, increases gradually to reach a steady value at 160 s, indicating that CF-TP10 concentration in the GUV membrane is raised with time to its steady value (Fig. 3c). On the other hand, the lumen intensity due to CF-TP10, I_{lumen}, is zero at the beginning, but after 200 s, it gradually grows with time to reach a significant value at 6 min (Fig. 3c). The increase in I_{lumen} due to CF-TP10 is caused by the binding of CF-TP10 to LUV membranes in the GUV lumen. These data indicate that first the binding of CF-TP10 to the GUV membranes increases its concentration in the membrane to reach a steady value, and then CF-TP10 enters the GUV lumen without pore formation. In contrast, I_{lumen} does not increase in the GUVs at 0 mV significantly, indicating no entry of CF-TP10 (Fig. 3b).

In this method, the entry of CPPs into GUV lumen at a specific time, t, is judged if $I_{lumen}(t)$ is larger than the threshold intensity of I_{lumen} (Moghal et al. 2018). Based on this criterion, we can calculate the fraction of GUVs, $P_{entry}(t)$, which CPPs enter before time t among all examined GUVs (hereafter, fraction of entry) (Islam et al. 2014a; Moghal et al. 2018). $P_{entry}(t)$ is a measure of the rate of entry of CPPs into the GUV lumen, V_{entry}. Figure 3d shows that P_{entry} (6 min) increases as $|\varphi_m|$ increases. Another measure of V_{entry}, I_{lumen} (6 min), also increases with increasing $|\varphi_m|$ (Fig. 3e). These results indicate that the V_{entry} of CF-TP10 without pore formation increases as $|\varphi_m|$ increases.

Accurate analysis of the I_{rim} due to CF-TP10, which is proportional to the CF-TP10 concentration in the GUV membrane, using GUVs not containing vesicles, provides information on the entry of CF-TP10 into vesicle lumen (Islam et al. 2014a). After the interaction of CF-TP10 with a single GUV at -59 mV starts, the I_{rim} grows gradually with time to attain a steady value, which is greater than that at 0 mV (Fig. 3f). Based on the analysis of our previous reports (Islam et al. 2014a, 2017; Moghal et al. 2018), the results of Fig. 3 c and f can be interpreted as follows; CF-TP10 binds to the outer leaflet of the GUV membrane from aqueous solution and then translocates from the outer leaflet to the inner leaflet (Fig. 1b). For 0.30–0.50-μM CF-TP10, the steady value of rim intensity increases with $|\varphi_m|$ (Fig. 3g). Figure 3h shows the φ_m dependence of the normalized I_{rim} (the ratio of I_{rim} at φ_m to I_{rim} at
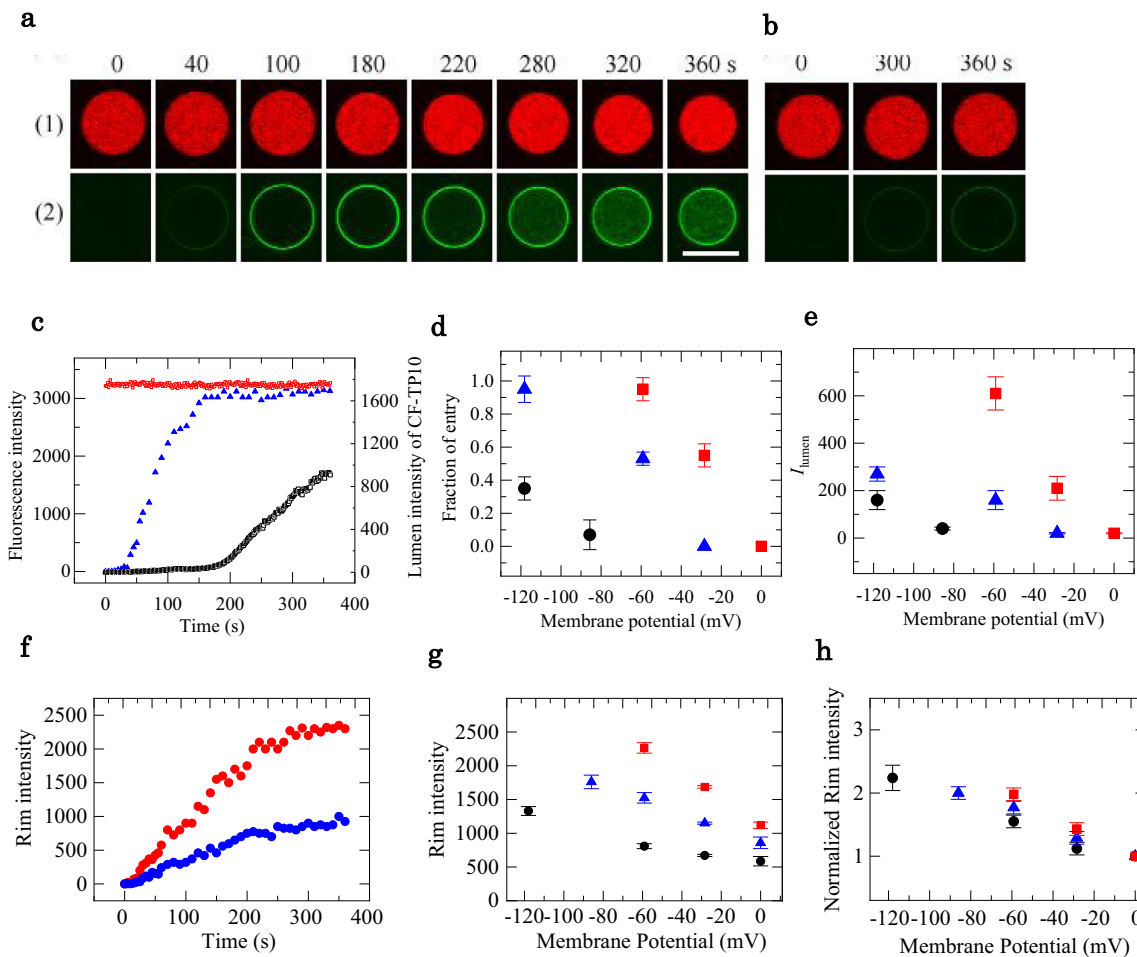
Fig. 3 Entry of CF-TP10 into single PG/PC (2/8)-GUVs under φ_m. **a, b** CLSM images due to (1) AF647 and (2) CF-TP10 of a GUV (containing LUVs in the GUV lumen) interacting with 0.50-μM CF-TP10 under $\varphi_m = -59$ mV (**a**) and 0 mV (**b**). The interaction time of CF-TP10 with a GUV is denoted by the numbers above each image. The bar denotes 20 μm. **c** Time course of the FI of the GUV shown in (**a**). I_{lumen} due to AF647 (red square), I_{rim} due to CF-TP10 (blue triangle), and the I_{lumen} due to CF-TP10 (black square). **d** The φ_m dependence of P_{entry} (6 min). (red square) 0.50 μM, (blue triangle) 0.40 μM, (black circle) 0.30 μM

CF-TP10 (same symbols are used in **e**, **g**, and **h**). **e** The φ_m dependence of I_{lumen} (6 min) without pore formation. **f** Time course change in I_{rim} of PG/PC (2/8)-GUV (not containing vesicles) interacting with 0.50 μM CF-TP10 under $\varphi_m = -59$ mV (red circle) and 0 mV (blue circle). **g** The φ_m dependence of I_{rim} due to CF-TP10. **h** The φ_m dependence of normalized I_{rim} due to CF-TP10. **a**, **b**, **c**, **d**, **e**, **f**, **g**, and **h** are reprinted with some modifications from Moghal et al. (2020) with permission from American Biophysical Society.

0 mV) is greater for higher CF-TP10 concentration. These results indicate that the CF-TP10 concentration in the GUV membrane increases with $|\varphi_m|$, mainly due to the growth of CF-TP10 concentration in the inner leaflet of the membrane (Moghal et al. 2020). We reasonably infer that the increase in CF-TP10 concentration in the inner leaflet with φ_m is one of the primary causes of the φ_m-induced increase in V_{entry}.

Conclusions and perspectives

This short review indicates that the effects of membrane potential on actions of LfcinB and CF-TP10 and the parts of their elementary processes are clearly revealed using the single GUV method. These studies have been just started. If we

use the advantage of the single GUV method (Islam et al. 2014b, 2018; Hasan and Yamazaki 2019; Hasan et al. 2019), we will get more information on the elementary processes of actions of AMPs and CPPs on membrane potential and their mechanisms in the near future. It is also necessary to investigate physical properties of GUVs under membrane potential using various methods and to use other methods of application of membrane potential to single GUVs.

We have a hypothesis that the structures of AMPs and natural CPPs have been improved by adapting to target cells to increase their activity during their long molecular evolution time, which is similar to the molecular evolution observed in viral membrane proteins (Pelkmans and Helenius 2003). If this hypothesis is true, there is a great possibility that these peptides utilize the membrane potential in cells to increase the

efficiency of their activities. As described in the Introduction, all live cells have membrane potential, whereas dead cells lose it. Thus, GUVs with membrane potential are more suitable as a model of cells or artificial cells, as well as GUVs containing small vesicles in the GUV lumen (Islam et al. 2014a; Moghal et al. 2018).

References

Alberts B, Johnson A, Lewis J, Morgan D, Raff M, Roberts K, Walter P (2015) Molecular biology of the cell, 6th edn. Garland Science, New York

Andersen OS (1983) Ion movement through gramicidin a channels: interfacial polarization effects on single-channel current measurements. Biophys J 41:135–146

Bechara C, Sagan S (2013) Cell-penetrating peptides: 20 years later, where do we stand? FEBS Lett 587:1693–1702

Bechniger B, Zasloff M, Opella SJ (1993) Structure and orientation of the antibiotic peptide magainin in membranes by solid-state nuclear magnetic resonance spectroscopy. Protein Sci 2:2077–2084

Bellamy W, Takase M, Yamauchi K, Wakabayashi H, Kawase K, Tomita M (1992) Identification of the bacterial domain of lactoferrin. Biochim Biophys Acta 1121:130–136

Blackiston DJ, McLaughlin KA, Levin M (2009) Bioelectric controls of cell proliferation. Cell Cycle 8:3527–3536

Bobone S, Stella L (2019) Selectivity of antimicrobial peptides; a complex interplay of multiple equilibria. In: Matsuzaki K (ed) Antimicrobial peptides: basic for clinical application. Springer, New York, pp 17–32

Christensen B, Fink J, Merrifield RB, Mauzerall D (1988) Channel-forming properties of cecropins and related model compounds incorporated into planar lipid membranes. Proc Natl Acad Sci U S A 85:5072–5076

Daniels CJ, Bole DG, Quay SC, Oxender DL (1981) Role for membrane potential in the secretion of protein into the periplasm of Escherichia coli. Proc Natl Acad Sci U S A 78:5396–5400

Dubey GP, Ben-Yehuda S (2011) Intercellular nanotubes mediate bacterial communication. Cell 144:590–600

EL-Andaloussi S, Johansson H, Magnusdottir A, Järver P, Lundberg P, Langel Ű (2005) TP10, a delivery vector for decoy oligonucleotides targeting the Myc protein. J Control Release 110:189–201

Fanghänel S, Wadhwani P, Strandberg E, Verdurmen WPR, Bűeck J, Ehni S, Mykhailiuk PK, Afonin S, Gerthsen D, Komarov IV, Brock R, Ulrich AS (2014) Structure analysis and conformational transitions of the cell penetrating peptide transportan 10 in the membrane-bound state. PLoS One 9:e99653

Felle H, Porter JS, Slayman CL, Kaback HR (1980) Quantitative measurements of membrane potential in Escherichia coli. Biochemistry 19:3585–3590

Finkelstein A, Andersen OS (1981) The gramicidin a channel: a review of its permeability characteristics with special reference to the single-file aspect of transport. J Membr Biol 59:155–171

Futaki S, Suzuki T, Ohashi W, Yagami T, Tanaka S, Ueda K, Sugiura Y (2001) Arginine-rich peptides. An abundant source of membrane-permeable peptides having potential as carriers for intracellular protein delivery. J Biol Chem 276:5836–5840

Gesell J, Zasloff M, Opella SJ (1997) Two-dimensional 1H NMR experiments show that the 23-residue magainin antibiotic peptide is an α-helix in dodecylphosphocholine micelles, sodium dodecylsulfate micelles, and trifluoroethanol/water solution. J Biomol NMR 9: 127–135

Hancock REW, Hans-Georg S (2006) Antimicrobial and host-defense peptides as new anti-infective therapeutic strategies. Nat Biotechnol 24:1551–1557

Hancock REW, Rozek A (2002) Role of membranes in the activities of antimicrobial cationic peptides. FEMS Microbiol Lett 206:143–149

Hasan M, Yamazaki M (2019) Elementary processes and mechanisms of interactions of antimicrobial peptides with membranes - single GUV studies. In: Matsuzaki K (ed) Antimicrobial peptides: basic for clinical application. Springer, New York, pp 17–32

Hasan M, Karal MAS, Levadnyy V, Yamazaki M (2018) Mechanism of initial stage of pore formation induced by antimicrobial peptide magainin 2. Langmuir 34:3349–3362

Hasan M, Moghal MMR, Saha SK, Yamazaki M (2019) The role of membrane tension in the action of antimicrobial peptides and cell-penetrating peptides in biomembranes. Biophys Rev 11:431–448

Henriques ST, Costa J, Castanho MARB (2005) Translocation of β-galactosidase mediated by the cell-penetrating peptide Pep-1 into lipid vesicles and human HeLa cells is driven by membrane electrostatic potential. Biochemistry 44:10189–10198

Hille B (1992) Ionic channels of excitable membranes, 2nd edn. Sinauer Association Inc, Massachusetts

Hossain F, Moghal MMR, Islam MZ, Moniruzzaman M, Yamazaki M (2019) Membrane potential is vital for rapid permeabilization of plasma membranes and lipid bilayers by the antimicrobial peptide lactoferricin B. J Biol Chem 294:10449–10462

Hwang PM, Zhou N, Shan X, Arrosmith CH, Vogel HJ (1998) Three-dimensional solution structure of lactoferricin B, an antimicrobial peptide derived from bovine lactoferrin. Biochemistry 37:4288–4298

Ishihara Y, Shimamoto N (2006) Involvement of endonuclease G in nucleosomal DNA fragmentation under sustained endogenous oxidative stress. J Biol Chem 281:6726–6733

Islam MZ, Ariyama H, Alam JM, Yamazaki M (2014a) Entry of cell-penetrating peptide transportan 10 into a single vesicle by translocating across lipid membrane and its induced pores. Biochemistry 53:386–396

Islam MZ, Alam JM, Tamba Y, Karal MAS, Yamazaki M (2014b) The single GUV method for revealing the functions of antimicrobial, pore-forming toxin, and cell-penetrating peptides or proteins. Phys Chem Chem Phys 16:15752–15767

Islam MZ, Sharmin S, Levadnyy V, Shibly SUA, Yamazaki M (2017) Effects of mechanical properties of lipid bilayers on entry of cell-penetrating peptides into single vesicles. Langmuir 33:2433–2443

Islam MZ, Sharmin S, Moniruzzaman M, Yamazaki M (2018) Elementary processes for the entry of cell-penetrating peptides into lipid bilayer vesicles and bacterial cells. Appl Microbiol Biotechnol 102:3879–3892

Kagan BL, Selsted ME, Ganz T, Lehrer R (1990) Antimicrobial defensin peptides from voltage-dependent ion-permeable channels in planar lipid bilayer membranes. Proc Natl Acad Sci U S A 87:210–214

Karal MAS, Alam JM, Takahashi T, Levadny V, Yamazaki M (2015) Stretch-activated pore of antimicrobial peptide Magainin 2. Langmuir 31:3391–3401

Kralj JM, Hochbaum DR, Douglass AD, Cohen AE (2011) Electrical spiking in Escherichia coli probed with a fluorescent voltage-indicating protein. Science 333:345–348

Kuwata H, Yip TT, Tomita M, Hutchens TW (1998) Direct evidence of the generation in human stomach of an antimicrobial peptide domain (lactoferricin) from ingested lactoferrin. Biochim Biophys Acta 1429:129–141

Lin C-C, Bachmann M, Bachler S, Venkatesan K, Dittrich PS (2018) Tunable membrane potential reconstituted in giant vesicles

promotes permeation of cationic peptides at nanomolar concentrations. ACS Appl Mater Interfaces 10:41909–41916

Madani F, Lindberg S, Langel Ű, Futaki S, Gräslund A (2011) Mechanisms of cellular uptake of cell-penetrating peptides. J Biophysics 414729

Martinac B, Buechner M, Delcour AH, Adler J, Kung C (1987) Pressure-sensitive ion channel in *Escherichia coli*. Proc Natl Acad Sci U S A 84:2297–2301

Melo MN, Ferre R, Castanho ARB (2009) Antimicrobial peptides: linking partition, activity and high membrane-bound concentrations. Nat Rev Microbiol 8:1–5

Moghal MMR, Islam MZ, Sharmin S, Levadnyy V, Moniruzzaman M, Yamazaki M (2018) Continuous detection of entry of cell-penetrating peptide Transportan 10 into single vesicles. Chem Phys Lipids 212:120–129

Moghal MMR, Islam MZ, Hossain F, Saha SK, Yamazaki M (2020) Role of membrane potential on entry of cell-penetrating peptide transportan 10 into single vesicles. Biophys J 118:57–60

Moniruzzaman M, Alam JM, Dohra H, Yamazaki M (2015) Antimicrobial peptide lactoferricin B-induced rapid leakage of internal contents from single giant unilamellar vesicles. Biochemistry 54:5802–5814

Moniruzzaman M, Islam MZ, Sharmin S, Dohra H, Yamazaki M (2017) Entry of a six-residue antimicrobial peptide derived from Lactoferricin B into single vesicles and *Escherichia coli* cells without damaging their membranes. Biochemistry 56:4419–4431

Pasupleti M, Schmidtchen A, Malmsten M (2012) Antimicrobial peptides: key components of the innate immune system. Crit Rev Biotechnol 32:143–171

Pautot S, Frisken BJ, Weitz DA (2003) Production of unilamellar vesicles using an inverted emulsion. Langmuir 19:2870–2879

Pelkmans L, Helenius A (2003) Insider information: what viruses tell us about endocytosis. Curr Opin Cell Biol 15:414–422

Propheter DC, Chara AL, Harris TA, Ruhn KA, Hooper LV (2017) Resistin-like molecule β is a bactericidal protein that promotes spatial segregation of the microbiota and the colonic epithelium. Proc Natl Acad Sci U S A 114:11027–11033

Richardson BD, Saha K, Krout D, Cabrera E, Felts B, Henry LK, Swant J, Zou M-F, Newman AH, Khoshbouei H (2015) Membrane potential shapes regulation of dopamine transporter trafficking at the plasma membrane. Nat Commun 7:10423

Rothbard JB, Jessop TC, Lewis RS, Murray BA, Wender PA (2004) Role of membrane potential and hydrogen bonding in the mechanism of translocation of guanidinium-rich peptides into cells. J Am Chem Soc 126:9506–9507

Rothbard JB, Jessop TC, Wender PA (2005) Adaptive translocation: the role of hydrogen bonding and membrane potential in the uptake of guanidinium-rich transporters into cells. Adv Drug Deliv Rev 57: 495–504

Ruthe H-J, Adler J (1985) Fusion of bacterial spheroplasts by electric fields. BBA-Biomembranes 819:105–113

Shapiro HM (1994) Cell membrane potential analysis. Methods Cell Biol 41:121–133

Sharmin S, Islam MZ, Karal MAS, Shibly SUA, Dohra H, Yamazaki M (2016) Effects of lipid composition on the entry of cell-penetrating peptide oligoarginine into single vesicles. Biochemistry 55:4154–4165

Shibly SUA, Ghatak C, Karal MAS, Moniruzzaman MM. Yamazaki M (2016) Experimental estimation of membrane tension induced by osmotic pressure. Biophys J 111:2190–2201

Sochacki KA, Barns KJ, Bucki R, Weisshaar JC (2011) Real-time attack on single Escherichia coli cells by the human antimicrobial peptide LL-37. Proc Natl Acad Sci U S A 108:E77–E81

Soomets U, Lindgren M, Gallet X, Pooga M, Hällbrink M, Elmquist A, Balaspiri L, Zorko M, Pooga M, Brasseur R, Langel Ű (2000) Deletion analogues of transportan. Biochim Biophys Acta 1467: 165–176

Sperelakis N (2012) Cell physiology source book, Essentials of membrane biophysics, 4th edn. Academic press, London

Stanzl EG, Trantow BM, Vargas JR, Wender PA (2013) Fifteen years of cell-penetrating, guanidinium-rich molecular transporters: basic science, research tools, and clinical applications. Acc Chem Res 46: 2944–2954

Strahl H, Hamoen LW (2010) Membrane potential is important for bacterial cell division. Proc Natl Acad Sci U S A 107:12281–12286

Stratford JP, Edwards CLA, Ghanshyam MJ, Malyshev D, Delise MA, Hayashi Y, Asally M (2019) Electrically induced bacterial membrane-potential dynamics correspond to cellular proliferation capacity. Proc Natl Acad Sci U S A 116:9552–9557

Sun Y, Sun T-L, Huang HW (2016) Mode of action of antimicrobial peptides on *E. coli* spheroplasts. Biophys J 111:132–139

Sunderacruz S, Levin M, Kaplan DL (2009) Role of membrane potential in the regulation of cell proliferation and differentiation. Stem Cell Rev Rep 5:231–246

Tamba Y, Yamazaki M (2005) Single giant unilamellar vesicle method reveals effect of antimicrobial peptide, magainin 2, on membrane permeability. Biochemistry 44:15823–15833

Tamba Y, Yamazaki M (2009) Magainin 2-induced pore formation in membrane depends on its concentration in membrane interface. J Phys Chem B 113:4846–4852

Tamba Y, Ohba S, Kubota M, Yoshioka H, Yoshioka H, Yamazaki M (2007) Single GUV method reveals interaction of tea catechin (−)-epigallocatechin gallate with lipid membranes. Biophys J 92:3178–3194

Tamba Y, Ariyama H, Levadny V, Yamazaki M (2010) Kinetic pathway of antimicrobial peptide magainin 2-induced pore formation in lipid membranes. J Phys Chem B 114:12018–12026

Tamba Y, Terashima H, Yamazaki M (2011) A membrane filtering method for the purification of giant unilamellar vesicles. Chem Phys Lipids 164:351–358

Terrone D, Sang SLW, Roudaia L, Silvius JR (2003) Penetratin and related cell-penetrating cationic peptides can translocate across lipid bilayers in the presence of a transbilayer potential. Biochemistry 42: 13787–13799

Walde P, Cosentino K, Engel H, Stano P (2010) Giant vesicles: preparations and applications. ChemBioChem 11:848–865

Wallbrecher R, Ackels T, Olea RA, Klein MJ, Caillon L, Schiller J, Bovée-Geurts PH, van Kuppevelt TH, Ulrich AS, Spehr M, Adjobo-Hermans MJW, Brock R (2017) Membrane permeation of arginine-rich cell-penetrating peptides independent of transmembrane potential as a function of lipid composition and membrane fluidity. J Control Release 256:68–78

Wei L, LaBouyer MA, Darling LEO, Elmore DE (2016) Bacterial spheroplasts as a model for visualizing membrane translocation of antimicrobial peptides. Antimicrob Agents Chemother 60:6350–6352

Wu M, Maier E, Benz R, Hancock REW (1999) Mechanism of interaction of different classes of cationic antimicrobial peptides with planar bilayers and with the cytoplasmic membrane of *Escherichia coli*. Biochemistry 38:7235–7242

Yamazaki M (2008) The single GUV method to reveal elementary processes of leakage of internal contents from liposomes induced by antimicrobial substances. Adv Planar Lipid Bilayers Liposomes 7: 121–142

Yeaman MR, Yount NY (2003) Mechanisms of antimicrobial peptide action and resistance. Pharmacol Rev 55:27–55

Yeaman MR, Bayer AS, Koo S-P, Foss W, Sullam PM (1998) Platelet microbicidal proteins and neutrophil defensing disrupt the

Staphylococcus aureus cytoplasmic membrane by distinct mechanism of action. J Clin Invest 101:178–187

Zasloff M (1987) Magainins, a class of antimicrobial peptides from Xenopus skin: isolation, characterization of two active forms, and partial cDNA sequence of a precursor. Proc Natl Acad Sci U S A 84: 5449–5453

Zasloff M (2002) Antimicrobial peptides of multicellular organisms. Nature 415:389–395

Zhang X, Jin Y, Plummer MR, Pooyan S, Gunaseelan S, Sinko PJ (2009) Endocytosis and membrane potential are required for Hela cell uptake of R.I.-CKTat9, a retro-inverso tat cell penetrating peptide. Mol Pham 6:836–848

Zhou Y, Wong C-O, Cho K-J, van der Hoeven D, Liang H, Thakur DP, Luo J, Babic M, Zinsmaier KE, Zhu MX, Hu H, Venkatachalam K, Hancock JF (2015) Membrane potential modulates plasma membrane phospholipid dynamics and K-Ras signaling. Science 349: 873–876

Zorko M, Langel Ű (2005) Cell-penetrating peptides: mechanism and kinetics of cargo delivery. Adv Drug Deliv Rev 57:529–545